Physiologic Changes in a Nonhuman Primate Model of HIV-Associated Pulmonary Arterial Hypertension

M. Patricia George[1,2], Hunter C. Champion[1,2], Marc Simon[1], Siobhan Guyach[3], Rebecca Tarantelli[3], Heather M. Kling[3], Alexandra Brower[6], Christopher Janssen[4], Jessica Murphy[3], Jonathan P. Carney[5], Alison Morris[1,3], Mark T. Gladwin[1,2], and Karen A. Norris[3]

[1]Department of Medicine, [2]Vascular Medicine Institute, [3]Department of Immunology, [4]Division of Laboratory Animal Resources, and [5]Department of Radiology, School of Medicine, University of Pittsburgh, Pittsburgh, Pennsylvania; and [6]School of Veterinary Medicine, University of Nottingham, Loughborough, England, United Kingdom

Pulmonary arterial hypertension (PAH) is increased in HIV, but its pathogenesis is not fully understood. Nonhuman primates infected with simian immunodeficiency virus (SIV) or SIV-HIV chimeric virus (SHIV) exhibit histologic changes characteristic of human PAH, but whether hemodynamic changes accompany this pathology is unknown. Repeated measurements of pulmonary artery pressures would permit longitudinal assessments of disease development and provide insights into pathogenesis. We tested the hypothesis that SIV-infected and SHIV-infected macaques develop physiologic manifestations of PAH. We performed right heart catheterizations, echocardiography, and computed tomography (CT) scans in macaques infected with either SIV (ΔB670) or SHIV (89.6P), and compared right heart and pulmonary artery pressures, as well as pulmonary vascular changes on CT scans, with those in uninfected control animals. Right atrial, right ventricular systolic, and pulmonary artery pressures (PAPs) were significantly elevated in 100% of macaques infected with either SIV or SHIV compared with control animals, with no difference in pulmonary capillary wedge pressure. PAPs increased as early as 3 months after SIV infection. Radiographic evidence of pulmonary vascular pruning was also found. Both SIV-infected and SHIV-infected macaques exhibited histologic changes in pulmonary arteries, predominantly consisting of intimal and medial hyperplasia. This report is the first to demonstrate SHIV-infected and SIV-infected macaques develop pulmonary hypertension at a high frequency, with physiologic changes occurring as early as 3 months after infection. These studies establish an important nonhuman primate model of HIV-associated PAH that will be useful in studies of disease pathogenesis and the efficacy of interventions.

Keywords: pulmonary hypertension; HIV; SIV; SHIV; macaque model

CLINICAL RELEVANCE

Pulmonary arterial hypertension (PAH) is a serious complication of HIV infection, and its pathogenesis is not fully understood. Nonhuman primate models of HIV infection using simian immunodeficiency virus (SIV) have been useful in understanding mechanisms of viral pathogenesis as well as sequelae of chronic infection. Several studies have shown that a percentage of SIV-infected and chimeric SIV-HIV (SHIV)–infected macaques develop pulmonary artery lesions, characterized by intimal thickening and luminal occlusion, with a histologic similarity to those associated with human PAH. However, the development of pulmonary arterial lesions cannot be predicted before an animal's death. Furthermore, the association of pulmonary arterial lesions and physiologic evidence of PAH in the SIV/SHIV model has not been reported. This report is the first to demonstrate the pulmonary hemodynamic and radiographic consequences of SIV and SHIV infections in macaques, and establishes an important nonhuman primate model of HIV-associated pulmonary hypertension. The ability to perform longitudinal physiologic measurements in SIV-infected or SHIV-infected macaques greatly expands the potential applicability of this model to both studies of disease pathogenesis and the efficacy of interventions.

HIV-infected individuals are at increased risk of pulmonary arterial hypertension (PAH), with a prevalence of 0.5 to 2.0% (1, 2). This prevalence has been unaffected by the development of combination antiretroviral therapy (3). Recent studies indicate that HIV-PAH may be even more common than previously thought (4–6). Associated with a 60% survival at 2 years after diagnosis, HIV-PAH involves even greater mortality in patients with more severe disease (World Health Organization Classes III–IV) (7). Although several reports have described clinical benefits with pulmonary hypertensive therapies in patients with HIV-PAH, it is still considered a terminal illness (8–11).

Animal models of PAH incompletely recapitulate critical elements of the pulmonary vascular remodeling seen in human disease, and this has constituted a major challenge in the field. Rodent models of PAH using monocrotaline or hypoxia have helped in understanding the pathogenesis of PAH, but these models do not replicate the potential contribution of the HIV virus to disease development (12, 13). Murine modeling of HIV and AIDS has developed to include transgenic and humanized rodent models. Although these models are useful, it is difficult to determine whether end-organ effects such as PAH are truly caused by HIV infection or by a phenomenon associated with the xenograft (14–16).

Simian immunodeficiency virus (SIV) and chimeric SIV-HIV viruses (SHIVs), generated by the insertion of HIV genes into the SIV backbone, have been used extensively in susceptible

(*Received in original form December 15, 2011 and in final form October 30, 2012*)

Author Contributions: All authors meet the International Committee of Medical Journal Editors criteria for authorship. All authors contributed to the conception and design, acquisition of data, or analysis and interpretation of data. All authors have contributed to the drafting or critical revision of the article for important intellectual content. All authors have approved the final version submitted for publication.

This research was supported by National Institute of Health grants R01 HL083462 and 5R01 HL077095 (K.A.N.), 3UL1RR024153–04S3 (H.C.C.), and P01 HL103455 (M.T.G, K.A.N., H.C.C., and A.M.), the Parker B. Francis Foundation (M.P.G.), the University of Pittsburgh Vascular Medicine Institute Program (M.P.G. and H.C.C.), and the Hemophilia Center of Western Pennsylvania (M.P.G. and H.C.C.).

Correspondence and requests for reprints should be addressed to Karen A. Norris, Ph.D., Department of Immunology, School of Medicine, University of Pittsburgh, 200 Lothrop Street, Pittsburgh, PA 15261. E-mail: kan1@pitt.edu.edu

This article has an online supplement, which is accessible from this issue's table of contents at www.atsjournals.org

Am J Respir Cell Mol Biol Vol 48, Iss. 3, pp 374–381, Mar 2013

Originally Published in Press as DOI: 10.1165/rcmb.2011-0434OC on December 13, 2012
Internet address: www.atsjournals.org

nonhuman primates for modeling HIV infection and for the preclinical testing of antiretroviral drugs and vaccine candidates (17, 18). As potential models of HIV-associated PAH, SIV-infected and SHIV-infected macaques may be particularly useful because they reflect a naturally occurring cause of human PAH (19, 20). Several studies have shown that SIV-infected and SHIV-infected macaques develop pulmonary artery lesions, characterized by intimal thickening and luminal occlusion, with histologic similarity to those associated with human PAH, but the development of pulmonary arterial lesions cannot be predicted before necropsy (19–21). Furthermore, the association of pulmonary arterial lesions and physiologic evidence of PAH in the SIV/SHIV model has not been reported. Hemodynamic assessment by right heart catheterization is the best means of definitively diagnosing PAH in humans and evaluating treatment efficacy (22). Here, we assessed the hemodynamic parameters of normal and SHIV-*envelope* (*env*)-infected cynomolgus macaques and SIV-infected rhesus macaques by right heart catheterizations and echocardiography, and evaluated the physiologic and radiographic data during disease progression.

MATERIALS AND METHODS

Adult cynomolgus (CM) and rhesus (RM) macaques, aged 6 to 10 years (please *see* Table E1 in the online supplement for further details), were obtained from national primate centers or vendors approved by the Division of Laboratory Animal Research at the University of Pittsburgh. Prestudy screening is detailed in the online supplement. Animal experiments were approved by the Institutional Animal Care and Use Committee of the University of Pittsburgh, and were performed in accordance with the provisions of the United States Animal Welfare Act.

SIV and SHIV Virus Infection

SHIV-CM model. Nineteen CMs were intravenously inoculated with $1 \times 10^{4.9}$ tissue culture infectious doses of $SHIV_{89.6P}$-*env* (gift of O. Narayan, University of Kansas) (23, 24). Healthy, uninfected CMs were used as controls.

SIV-RM model. Four RMs were intrarectally inoculated with SIV ΔB670 (gift of M. Murphey-Corb, University of Pittsburgh). Plasma viral loads and peripheral blood $CD4^+$ T cells were determined by quantitative RT-PCR and flow cytometry (24, 25). Age, clinical, and infection parameters are presented in the online supplement.

Hemodynamic Measurements

SHIV-CM model. Four uninfected CMs and 19 SHIV-infected CMs underwent right heart catheterization (RHC) at 19–22 months after infection. In seven SHIV-infected CMs, simultaneous pulmonary artery pressure and Doppler blood flow were measured, and pulmonary vascular resistance (PVR) and cardiac output were calculated (26).

SIV-RM model. Two-dimensional Doppler echocardiography and RHC were performed before infection, and repeated at 3 months (echocardiography) and 8 months (RHC) after infection. Systemic blood pressure measurements were obtained before infection and after infection at monthly intervals. Detailed methods are presented in the online supplement.

Quantification of Small Pulmonary Vessels by Computed Tomography

Computed tomography (CT) scan images were obtained on uninfected CMs and SHIV-infected CMs at 19–22 months after infection. To quantify small-vessel pruning, noncontrast CT scans were analyzed by the method described by Matsuoka and colleagues to quantify the cross-sectional area (CSA) of pulmonary vessels (27). Additional details are provided in the online supplement.

Tissue and Histologic Examination

Lung tissue was obtained during necropsy, and pulmonary arteries were examined by a pulmonologist and a veterinary pathologist (M.P.G. and A.B., respectively) blinded to the identity of the monkeys, as previously described (21, 28) (further details are available in the online supplement).

Statistical Analysis

Hemodynamic parameters were compared between SHIV-infected and uninfected CMs, using the Wilcoxon-Mann-Whitney test. A paired *t* test was used to compare hemodynamic parameters before and after the SIV infection of RMs. Mean percent CSAs were compared between SHIV-infected and uninfected CMs, using a two-tailed *t* test. Relationships between hemodynamic measurements and histology, $CD4^+$ T cell count, viral concentrations, and the presence of histologic lesions were determined using the Wilcoxon-Mann-Whitney test, the Spearman correlation, and linear regression.

RESULTS

Infection of Cynomolgus Macaques with $SHIV_{89.6P}$ Is Associated with Elevations in Right-Sided Pressures and Pulmonary Artery Pressures

Normal and $SHIV_{89.6P}$-infected CMs were evaluated for physiologic and anatomic evidence of PAH (*see* Table E1 and Figure E1 for viral loads and peripheral blood CD4 T-cell concentrations). At 19–24 months after infection, macaques underwent right heart catheterization (Table E2). The median age at time of catheterization was 9.35 years (range, 7.49–9.62 yr) in SHIV-infected animals, and 6.60 years (range, 6.17–7.32 yr) in control animals. Right atrial pressure (RAP) and right ventricular systolic pressure (RVSP) were elevated in SHIV-infected macaques compared with uninfected control animals (median RAP, 4 mm Hg; range, 3–7 mm Hg in SHIV animals, versus 2 mm Hg; range, 2–3 mm Hg in control animals; $P = 0.001$; median RVSP, 14 mm Hg; range, 10–38 mm Hg in SHIV animals, versus 9 mm Hg; range, 8–9 mm Hg in control animals; $P = 0.042$; Figure 1; see Table E2 in the online supplement for hemodynamic values of individual animals). Pulmonary artery systolic and diastolic pressures (PASP and PADP, respectively) were also elevated in SHIV-infected macaques compared with control animals (median PASP, 14 mm Hg; range, 10–22 mm Hg, versus 8 mm Hg; range, 7–9 mm Hg; $P = 0.002$; median PADP, 9 mm Hg; range, 5–12 mm Hg, versus 4.5 mm Hg; range, 4–5 mm Hg; $P = 0.004$). Calculated mean pulmonary arterial pressure (mPAP) was elevated in SHIV-infected macaques compared with control animals (median mPAP, 10 mm Hg; range, 7–5 mm Hg in SHIV animals, versus 5.5 mm Hg; range, 5–6 mm Hg in control animals; $P = 0.001$; Figure 1). No significant difference was evident regarding pulmonary capillary wedge pressure (PWCP) in SHIV-infected macaques versus control animals (median PCWP, 3 mm Hg; range, 2–4 mm Hg in SHIV-infected animals, versus 2.5 mm Hg; range, 2–3 mm Hg in control animals; $P = 0.27$; Figure 1).

Infection with SHIV Is Associated with Decreased Vascular Compliance and Increased Pulmonary Vascular Resistance

In addition to the overall increase in right-sided pressures, the contour of the RVSP waveform in infected animals was notably different than the waveform in uninfected control animals (Figure 2). In SHIV-infected animals, a loss of the gentle sloping of the shoulder in the end systolic waveform seen after peak RVSP was evident, indicative of increased vascular stiffness (Figure 2, *arrow*) (29). This pattern was not seen in uninfected animals.

To identify whether increased RAP, RVSP, and pulmonary artery pressures were attributable to increased pulmonary arterial tone or secondary to left heart dysfunction, we measured intra-arterial flow and Doppler pressures in a subset of animals (four SHIV-infected and three uninfected; see the online supplement for further details). PVR was increased in 4/4 SHIV-infected animals (mean, 0.18 Woods units; 95% confidence interval [CI],

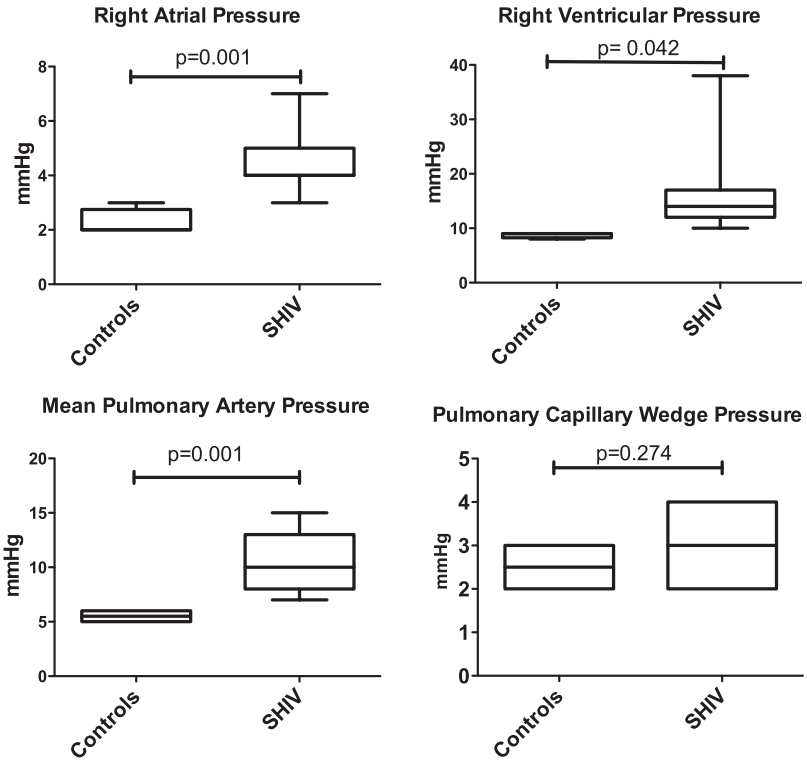

Figure 1. Infection of cynomolgus macaques with simian immunodeficiency virus–human immunodeficiency virus 89.6P ($SHIV_{89.6P}$) is associated with elevated right atrial, right ventricular, and pulmonary arterial pressures (Mann-Whitney test, $P = 0.001$, 0.042, and 0.001, respectively), but not pulmonary capillary wedge pressure (Mann-Whitney test, $P = 0.274$). Right heart catheterizations were performed in 19 macaques, at approximately 20 months after SHIV infection, and compared with four uninfected control animals.

0.09–0.28), relative to uninfected control animals (mean, 0.06 Woods units; 95% CI, 0.03–0.09; $P = 0.02$; Figure 3). Of note, no difference was evident in the relative cardiac output of these animals (mean pulmonary flow of 53.3 cm/s; 95% CI, 39.5–67 cm/s in SHIV-infected animals, versus mean pulmonary flow of 57 cm/s; 95% CI, 49.6–64.5 cm/s in control animals; $P = 0.51$). Pulmonary pressures were not associated with CD4 nadirs or viral loads, which function as indices of SHIV infection severity (data not shown).

Infection of Rhesus Macaques with $SIV_{\Delta B670}$ Is Associated with Elevations in Right-Sided Pressure and Pulmonary Artery Pressure

Compared with the SHIV infection of CMs, which induces a rapid loss of peripheral blood $CD4^+$ T cells but relatively mild disease, SIV infection of RMs typically results in a gradual loss of peripheral blood $CD4^+$ T cells, higher sustained plasma viral loads, and the development of AIDS-like disease (30) (please see Figure E1 in the online supplement). Thus, we sought to

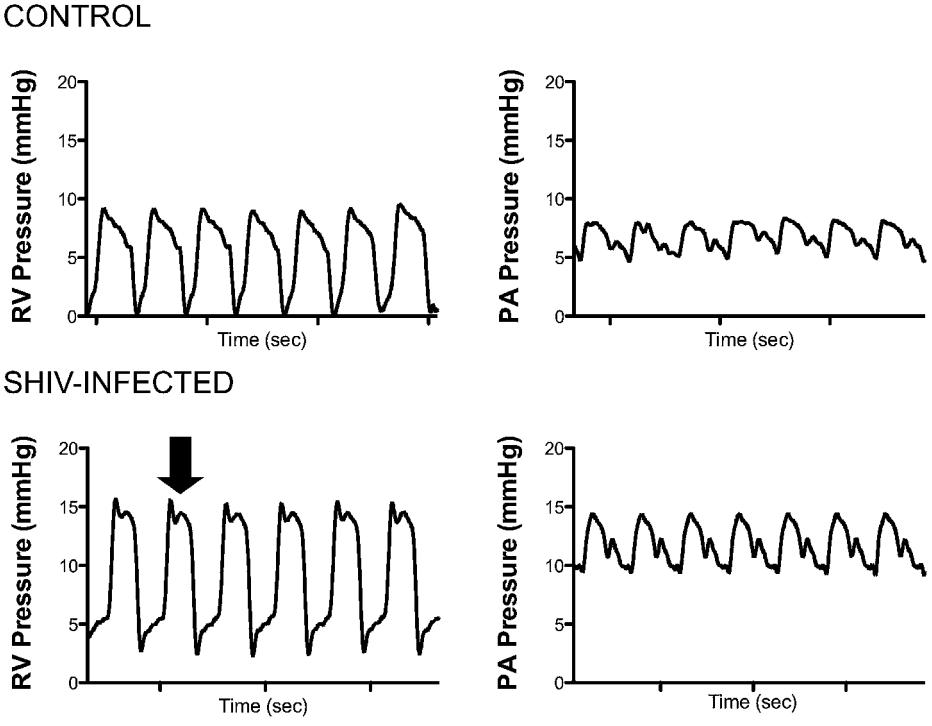

Figure 2. Right ventricle (RV) pressure waveform morphology is consistent with stiffening of the vasculature. *Arrow* indicates a loss of the gentle sloping of the shoulder during systole after peak right ventricular systolic contraction, consistent with increased vascular tone. RV, right ventricle; PA, pulmonary artery.

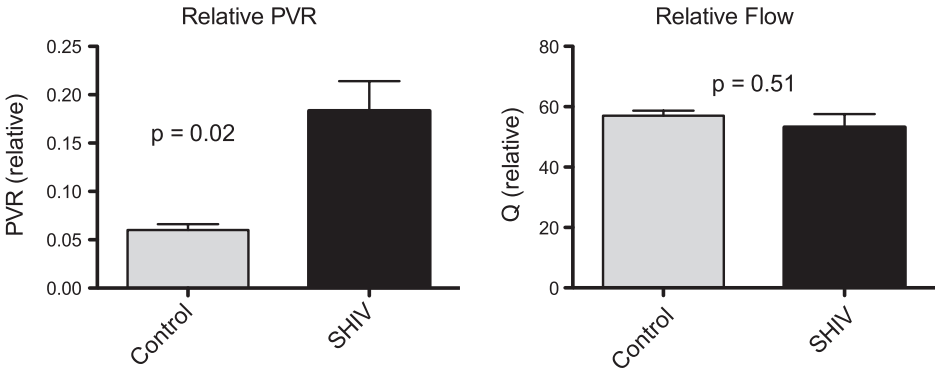

Figure 3. Relative pulmonary vascular resistance (PVR, Woods units) is elevated in SHIV-infected macaques ($n = 4$) compared with uninfected macaques ($n = 3$; $P = 0.02$), with no significant difference in relative cardiac output (Q, blood flow [cm/s]; $P = 0.51$) ($P = 0.51$).

determine whether the hemodynamic changes observed in the SHIV-CM model also occurred in SIV-infected RMs. As determined by Doppler echocardiography, pulmonary arterial systolic pressure was significantly elevated in RMs by 3 months after SIV infection ($P = 0.036$; Figure 4A). Further elevations of right atrial and pulmonary arterial pressures were observed at 8 months after infection, as determined by RHC (Figure 4B), with no significant difference in PCWP ($P = 0.215$). No significant changes in systemic blood pressure were detected before and after SIV infection ($P = 0.903$; Figure 4C). One SIV-infected RM (R85) was killed before the 8-month RHC because of SIV disease progression.

Radiographic Evidence of Alteration in the Small Vessels among SHIV-Infected Macaques

CT evidence of the pulmonary vascular pruning of small pulmonary vessels was seen in 19 SHIV-infected macaques, compared with 10 uninfected control animals. The percent CSA in vessels less than 5 mm^2 (percent $CSA_{<5\ mm2}$) was significantly lower in SHIV-infected animals (mean, 0.87%; SD, ± 0.1%) compared with control animals (mean, 1.0%; SD, ± 0.3%; $P = 0.04$), indicative of pulmonary arterial pruning. No significant difference was evident between SHIV-infected and control animals with regard to the percent CSA of vessels 5–10 mm^2 in size ($P = 0.45$; Figure 5).

Histopathological Lesions Were Present in SHIV-Infected Macaques

Pulmonary vascular lesions were seen in SHIV-infected CMs and in SIV-infected RMs (Figure 6 and Table E2). The predominant lesions involved intimal and medial hyperplasia of the medium arteries, and intramural fibrosis and perivascular lymphocytic infiltration, as previously reported in SIV-infected and SHIV-infected macaques (21) (Figure 6). RVSP and mPAP did not differ between animals with and without pulmonary vascular lesions (median RVSP in animals with lesions, 13.5 mm Hg; range, 10–20 mm Hg; median RVSP in animals without lesions, 14 mm Hg; range, 11–38 mm Hg; median mPAP in animals with lesions, 11 mm Hg; range, 7–15 mm Hg; median mPAP in animals without lesions, 10 mm Hg; range, 8–14 mm Hg).

DISCUSSION

We evaluated two nonhuman primate models of HIV infection for physiologic evidence of pulmonary hypertension. We report hemodynamic and radiographic changes and pulmonary vascular lesions in both SIV-infected and SHIV-infected macaques, consistent with those seen in human PAH. The most striking feature of the SIV and SHIV models is that 100% of the infected monkeys (cynomolgus and rhesus) exhibit elevated right heart and pulmonary arterial pressures as determined by RHC, and evidence of hemodynamic alterations as early as 3 months after infection in the SIV-infected macaques. No increase was evident in either PCWP or systemic blood pressure, or decrements in the cardiac output of infected animals, indicating that the pulmonary vascular changes seen were not the result of left-sided heart failure. Infected animals also demonstrated an increase in PVR compared with control animals, but with no significant difference in cardiac output. Using quantitative analyses of CT scans, SHIV-infected animals demonstrated evidence of pruning of the small pulmonary vessels. Together with anatomic evidence of pulmonary vasculopathy presented here and in previous studies of SIV-infected and SHIV-infected primates, these results provide compelling evidence that the SIV and SHIV infection of macaques induces PAH at a relatively high frequency (19–21). The ability to perform percutaneous measurements of right heart pressures in this model greatly expands its utility in tracking early events in PAH pathogenesis, the progression of disease, and responses to therapy.

In humans, PAH is defined as a sustained elevation of mPAP greater than 25 mm Hg at rest or 30 mm Hg with exercise, without elevations in PCWP (a marker of left ventricular dysfunction). In the primate models described here, we demonstrate that in both SHIV-infected CMs and SIV-infected RMs, all animals developed significantly elevated mPAP without elevations in PCWP, as well as elevated RAP and RVSP, indicative of a right heart/precapillary pulmonary artery disease process. These hemodynamic data were further supported by analyses of right ventricular waveforms. The loss of gentle sloping of the shoulder in the RVSP systolic waveform, seen only in the infected macaques, suggests increased vascular wave reflection in the infected animals (i.e., increased pulmonary arterial stiffness) (29). These increases in vascular pressures and tone in this model are consistent with PAH.

To evaluate disease progression further, using a noninvasive technique, we measured vascular changes in SHIV-infected animals with CT scans. We found significant evidence of pruning of the small vessels in SHIV-infected animals compared with uninfected control CMs. Although we did not have corresponding hemodynamic data in the control animals to explore direct correlations between pulmonary pressures and vascular pruning, these data suggest a process of increased vascular tone and/or remodeling when animals are infected with SHIV. This is the first report of radiologic evidence of vascular pruning in a nonhuman primate model of PAH.

All SHIV-infected and SIV-infected animals exhibited increased measurements of right heart and pulmonary artery pressure compared with control animals, but histologic evidence of vascular remodeling was not detected in all animals. Histopathological changes observed in the SHIV-infected macaques were relatively mild compared with those in SIV-infected macaques,

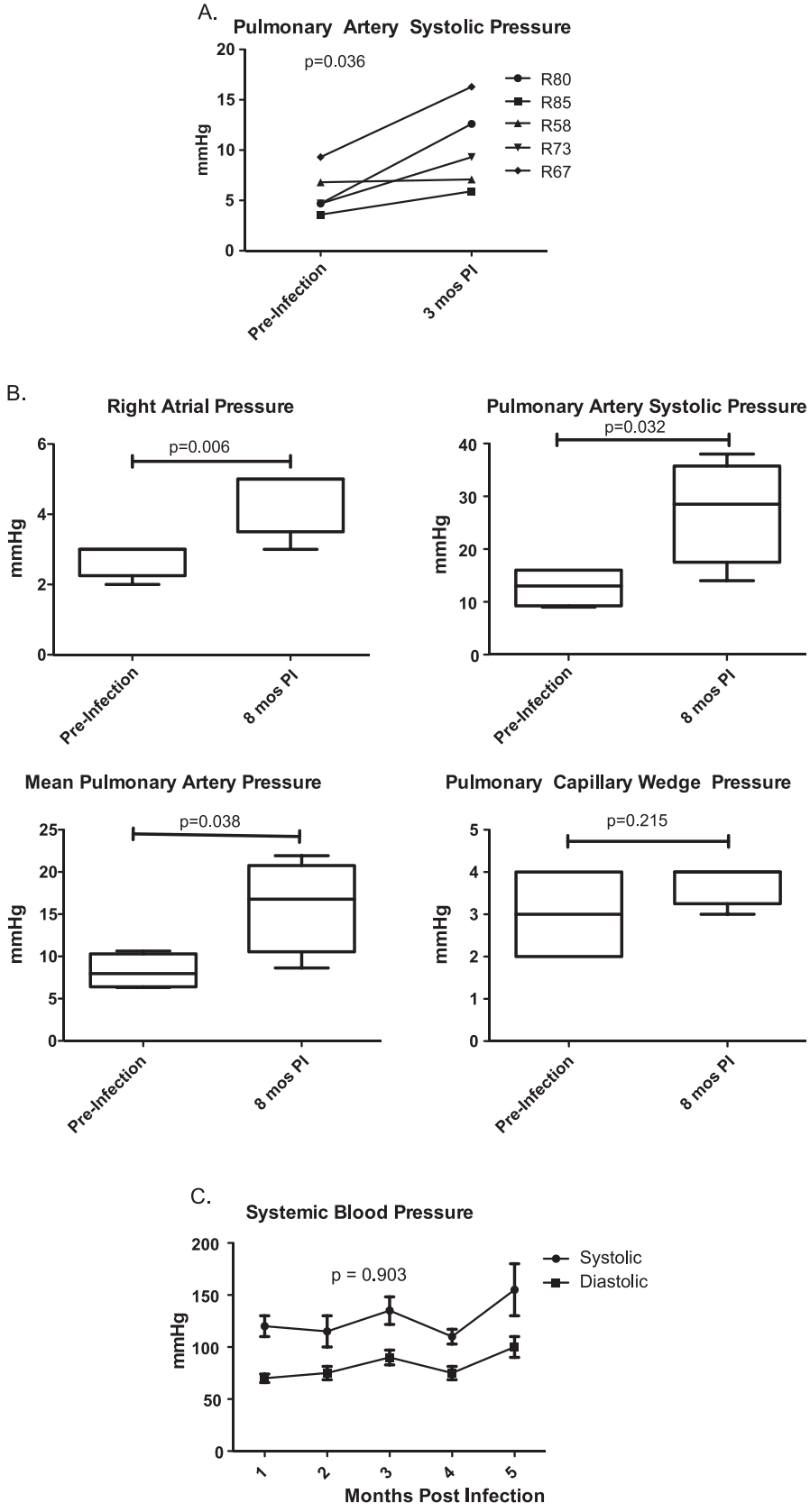

Figure 4. Hemodynamic evaluation of simian immunodeficiency virus (SIV)–infected rhesus macaques (Monkey numbers R58, R67, R73, R80, R85; *see* Table E1 for infection details). (*A*) Pulmonary artery systolic pressure is significantly elevated in rhesus macaques (RM) by 3 months post-SIV infection (PI) compared with baseline, as determined by Doppler echocardiography (two-way ANOVA, $P = 0.023$). Right heart catheterizations were performed in four rhesus macaques at baseline (before infection) and approximately 8 months after infection (PI). (*B*) Infection with $SIV_{\Delta B670}$ is associated with elevated right atrial and pulmonary artery pressure and pulmonary artery systolic pressure (paired *t* test, $P = 0.006$, 0.032, and 0.038, respectively), but not pulmonary capillary wedge pressure ($P = 0.215$). (*C*) No significant difference was evident in systemic blood pressure before and after SIV infection (two-way ANOVA, $P = 0.903$). mos, months.

suggesting that the severity of SIV infection may contribute to the development of more severe pulmonary hypertension (PH). As previously reported, SHIV and SIV infections resulted in less severe pathological changes compared with clinical PAH or some rodent models of PAH, perhaps consistent with early disease in primate models. Hence, although evidence of vascular remodeling exists in macaque models of PAH, physiologic changes and evidence of increases in vascular tone are

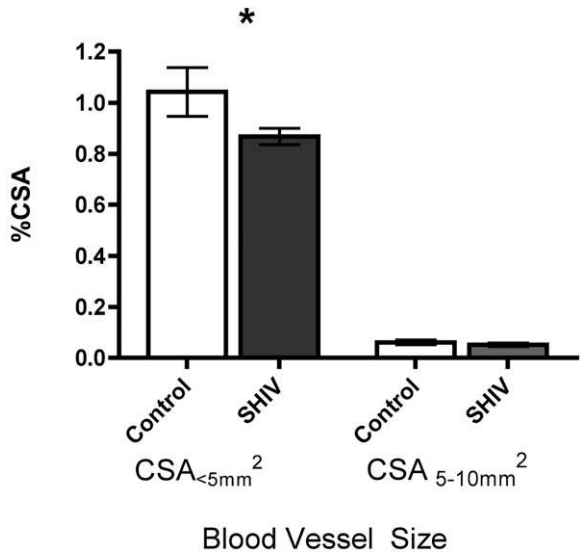

Figure 5. Quantitative evidence of vascular pruning on computed tomography scans. Quantitative analysis of cross-sectional area (CSA) of vessels was performed, and indicated significantly fewer small vessels (CSA < 5 mm^2) in SHIV-infected macaques ($n = 19$) than in control animals ($n = 10$; t test, $P = 0.041$). No significant difference was evident in vessels measuring 5–10 mm^2 (t test, $P = 0.450$). %CSA, percentage of cross-sectional area; $CSA_{<5\ mm^2}$, vessels with cross-sectional area < 5 mm^2; $CSA_{5–10\ mm^2}$, vessels with a cross-sectional area of 5–10 mm^2. *$P = 0.04$.

more prominent characteristics of this model. We do not know whether SHIV-infected or SIV-infected macaques will develop more significant lesions over time, as seen previously in other animal models, but increases in vascular tone may lead to downstream neointimal formation and arterial remodeling (13, 31).

Interestingly, in this study, 7/19 (37%) SHIV-infected macaques developed lesions, compared with 8/13 (62%) in our previous study (21). Although no significant difference was evident in the ages of the animals between the two cohorts, they were different in terms of gender composition (five females in the previous cohort, and none in the current SHIV cohort) and country of origin (the previous cohort was of Chinese origin, whereas the current SHIV cohort was predominantly from Mauritius, i.e., 16 animals from Mauritius, and three from China). The sex of the animals and their origin may play a role in their susceptibility to develop pathologic lesions of PAH.

Several studies have implicated HIV proteins in the pathogenesis of pulmonary vascular injury (20, 32, 33). We did not find a correlation between mPAP and peak plasma viral loads. Similarly, we did not see a correlation between CD4 nadirs and mPAP. These results are consistent with our earlier observation that the extent of pulmonary vascular pathology does not correlate with plasma viral loads or disease severity in SHIV-infected macaques (21). Further studies are needed to determine if a higher, sustained plasma viral set-point (as seen in the SIV-RM model) is associated with more severe pathology compared with SHIV-infected CMs. These findings do not necessarily exclude the possibility that specific viral proteins play a role in the pathogenesis of PAH, as suggested by other models (20, 34).

The nonhuman primate models of HIV-PAH described here have several potential advantages over previous animal models. First, viral infection is the sole precipitant agent of disease. Unlike other animal models of PAH, this model does not require hypoxia, monocrotaline, or other noxious stimuli to induce disease, potentially making it more physiologically relevant. Second, the nonhuman primate model may be more reflective of

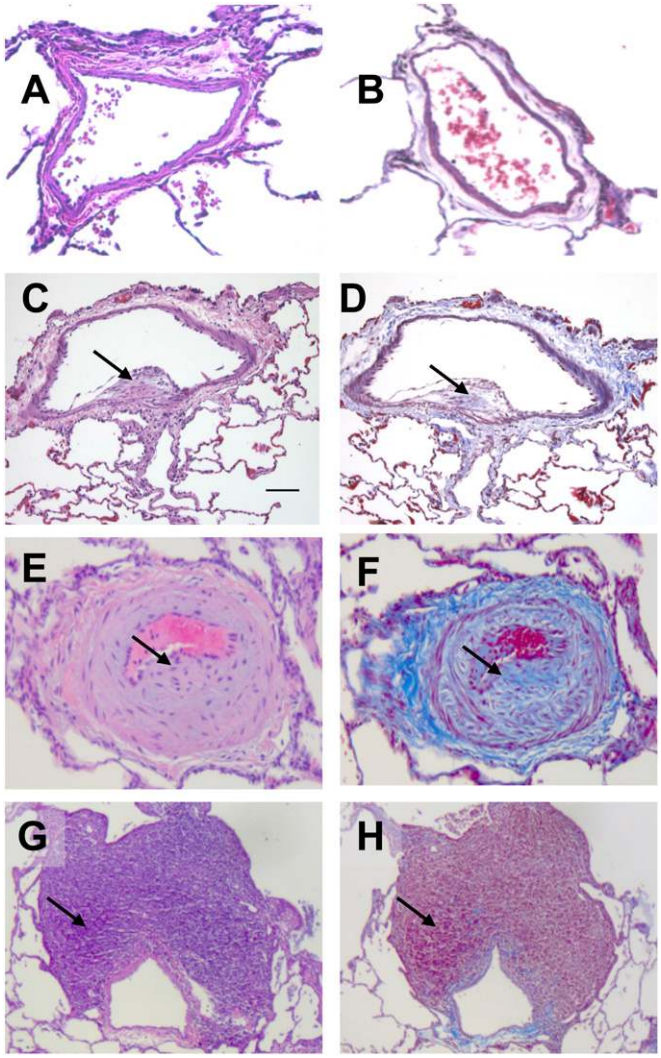

Figure 6. Characteristic histopathology of SHIV-infected and SIV-infected macaque lung tissue. Hematoxylin and eosin stain (*A*, *C*, *E*, and *G*) and Masson trichrome stain (*B*, *D*, *F*, and *H*) of normal (*A* and *B*), SHIV-infected (*C* and *D*), and SIV-infected (*E–H*) macaque lung tissue. *Arrows* indicate neointimal thickening (*C*), medial hyperplasia (*E*), collagen deposition (*F*), and perivascular lymphocytic tissue (*G*).

human disease compared with rodent models of pulmonary hypertension, given our evolutionary relationship to nonhuman primates. The increases of pressure were seen in all infected macaques, and are proportionally on par with those seen in humans with PAH. SHIV-infected macaques demonstrated an 83% greater mPAP compared with uninfected control animals (11 versus 6 mm Hg, respectively), comparable with the percent difference in mPAP among patients with documented PAH compared with normal individuals ($\sim$ 78.6%, with 25 mm Hg considered diagnostic of PAH, and with an average normal mPAP of 14 mm Hg) (35). Third, the SIV and SHIV infection of macaques comprises a well-characterized, reproducible model of HIV infection (24, 28, 36), and results in elevated right heart and pulmonary artery pressures in all infected animals. In addition, physiologic changes are seen before the onset of severe immunodeficiency in these animals. Finally, with the performance of right heart catheterizations, we expand the ability to track longitudinal disease progression in this model.

Our study contained several limitations. First, we evaluated pulmonary hemodynamics at a single time point after SHIV infection.

Serial measures of right heart and pulmonary pressures are now possible using this technique, and will establish important parameters associated with the development of vascular changes. Second, pulmonary pressure measurements were not available in our control animals used for radiologic analyses, so we were unable to perform correlation studies. Third, we saw relatively low pressures in both uninfected and infected cynomolgus and rhesus macaques, which may be an attribute of these species or an effect of the inhaled anesthetic used in the procedure (37, 38). In addition, the $SHIV_{89.6P}$ infection of CMs results in a rapid depletion of peripheral blood $CD4^+$ T cells. However, plasma viral concentrations are reduced relatively quickly compared with other models of SIV and SHIV infection (30). Thus, further studies with the SIV-RM model may produce different pathologic outcomes with respect to the development of PAH. This study did not address the multiple mechanisms whereby chronic viral infection leads to the development of pulmonary vascular remodeling and hypertension. Chronic immune activation and inflammation are well described in HIV-infected individuals and in susceptible macaques infected with SIV (39–42). We previously reported inflammatory cytokine production in SHIV-infected macaques (28), and we observed a trend toward increases in plasma inflammatory mediators in the current cohort of SIV-infected macaques (IL-8 and regulated on activation, T cell expressed and secreted; data not shown), although these increases were not statistically significant, possibly because of the small group size. A comprehensive analysis of immune activation and chronic inflammation associated with SIV infection and the development of PAH is underway. Moreover, the impact of direct viral interaction with the vasculature has been implicated in HIV-PAH. The viral proteins Nef, Tat, and Env were reported to be associated with endothelial cell dysfunction and smooth muscle cell hyperplasia (20, 32, 43), and may contribute to the development of PAH reported here.

In conclusion, we have described the first physiologic and radiographic characterization of experimental HIV-related pulmonary hypertension in nonhuman primates. Our findings suggest that in nonhuman primate models of HIV-PAH, increases in right heart and pulmonary arterial pressures and vascular tone occur at high frequency and relatively early after viral infection. The ability to perform longitudinal physiologic measurements in SIV-infected or SHIV-infected macaques greatly expands the potential applicability of this model to both primary mechanistic investigations of PAH, as well as preclinical drug testing.

Author disclosures are available with the text of this article at www.atsjournals.org.

References

1. Speich R, Jenni R, Opravil M, Pfab M, Russi EW. Primary pulmonary hypertension in HIV infection. *Chest* 1991;100:1268–1271.
2. Sitbon O, Lascoux-Combe C, Delfraissy JF, Yeni PG, Raffi F, De Zuttere D, Gressin V, Clerson P, Sereni D, Simonneau G. Prevalence of HIV-related pulmonary arterial hypertension in the current antiretroviral therapy era. *Am J Respir Crit Care Med* 2008;177:108–113.
3. Cicalini S, Almodovar S, Grilli E, Flores S. Pulmonary hypertension and human immunodeficiency virus infection: epidemiology, pathogenesis, and clinical approach. *Clin Microbiol Infect* 2011;17:25–33.
4. Morris A, Gingo MR, George MP, Lucht L, Kessinger C, Singh V, Hillenbrand M, Busch M, McMahon D, Norris KA, *et al*. Cardiopulmonary function in individuals with HIV infection in the antiretroviral therapy era. *AIDS* 2012;26:731–740.
5. Mondy KE, Gottdiener J, Overton ET, Henry K, Bush T, Conley L, Hammer J, Carpenter CC, Kojic E, Patel P, *et al*. High prevalence of echocardiographic abnormalities among HIV-infected persons in the era of highly active antiretroviral therapy. *Clin Infect Dis* 2011;52:378–386.
6. Hsue PY, Deeks SG, Farah HH, Palav S, Ahmed SY, Schnell A, Ellman AB, Huang L, Dollard SC, Martin JN. Role of HIV and human herpesvirus–8 infection in pulmonary arterial hypertension. *AIDS* 2008;22:825–833.
7. Nunes H, Humbert M, Sitbon O, Morse JH, Deng Z, Knowles JA, Le Gall C, Parent F, Garcia G, Herve P, *et al*. Prognostic factors for survival in human immunodeficiency virus–associated pulmonary arterial hypertension. *Am J Respir Crit Care Med* 2003;167:1433–1439.
8. Recusani F, Di Matteo A, Gambarin F, D'Armini A, Klersy C, Campana C. Clinical and therapeutical follow-up of HIV-associated pulmonary hypertension: prospective study of 10 patients. *AIDS* 2003;17:S88–S95.
9. Ghofrani HA, Friese G, Discher T, Olschewski H, Schermuly RT, Weissmann N, Seeger W, Grimminger F, Lohmeyer J. Inhaled iloprost is a potent acute pulmonary vasodilator in HIV-related severe pulmonary hypertension. *Eur Respir J* 2004;23:321–326.
10. Sitbon O, Gressin V, Speich R, Macdonald PS, Opravil M, Cooper DA, Fourme T, Humbert M, Delfraissy JF, Simonneau G. Bosentan for the treatment of human immunodeficiency virus–associated pulmonary arterial hypertension. *Am J Respir Crit Care Med* 2004;170:1212–1217.
11. Barbaro G, Lucchini A, Pellicelli AM, Grisorio B, Giancaspro G, Barbarini G. Highly active antiretroviral therapy compared with HAART and bosentan in combination in patients with HIV-associated pulmonary hypertension. *Heart* 2006;92:1164–1166.
12. Rabinovitch M, Gamble W, Nadas AS, Miettinen OS, Reid L. Rat pulmonary circulation after chronic hypoxia: hemodynamic and structural features. *Am J Physiol* 1979;236:H818–H827.
13. Okada K, Tanaka Y, Bernstein M, Zhang W, Patterson GA, Botney MD. Pulmonary hemodynamics modify the rat pulmonary artery response to injury: a neointimal model of pulmonary hypertension. *Am J Pathol* 1997;151:1019–1025.
14. Shacklett BL. Can the new humanized mouse model give HIV research a boost? *PLoS Med* 2008;5:e13.
15. Rahim MM, Chrobak P, Hu C, Hanna Z, Jolicoeur P. Adult AIDS-like disease in a novel inducible human immunodeficiency virus Type 1 Nef transgenic mouse model: $CD4^+$ T-cell activation is Nef dependent and can occur in the absence of lymphophenia. *J Virol* 2009;83:11830–11846.
16. Van Duyne R, Pedati C, Guendel I, Carpio L, Kehn-Hall K, Saifuddin M, Kashanchi F. The utilization of humanized mouse models for the study of human retroviral infections. *Retrovirology* 2009;6:76.
17. Joag SV. Primate models of AIDS. *Microbes Infect* 2000;2:223–229.
18. Hu SL. Non-human primate models for AIDS vaccine research. *Curr Drug Targets Infect Disord* 2005;5:193–201.
19. Chalifoux LV, Simon MA, Pauley DR, MacKey JJ, Wyand MS, Ringler DJ. Arteriopathy in macaques infected with simian immunodeficiency virus. *Lab Invest* 1992;67:338–349.
20. Marecki JC, Cool CD, Parr JE, Beckey VE, Luciw PA, Tarantal AF, Carville A, Shannon RP, Cota-Gomez A, Tuder RM, *et al*. HIV-1 Nef is associated with complex pulmonary vascular lesions in SHIV-Nef–infected macaques. *Am J Respir Crit Care Med* 2006;174:437–445.
21. George MP, Brower A, Kling H, Shipley T, Kristoff J, Reinhart TA, Murphey-Corb M, Gladwin MT, Champion HC, Morris A, *et al*. Pulmonary vascular lesions are common in SIV- and SHIV-*env*–infected macaques. *AIDS Res Hum Retroviruses* 2011;27:103–111.
22. Galie N, Hoeper MM, Humbert M, Torbicki A, Vachiery JL, Barbera JA, Beghetti M, Corris P, Gaine S, Gibbs JS, *et al*. Guidelines for the diagnosis and treatment of pulmonary hypertension: the Task Force for the Diagnosis and Treatment of Pulmonary Hypertension of the European Society of Cardiology (ESC) and the European Respiratory Society (ERS), endorsed by the International Society of Heart and Lung Transplantation (ISHLT). *Eur Heart J* 2009;30:2493–2537.
23. Reimann KA, Li JT, Veazey R, Halloran M, Park IW, Karlsson GB, Sodroski J, Letvin NL. A chimeric simian/human immunodeficiency virus expressing a primary patient human immunodeficiency virus Type 1 isolate *env* causes an AIDS-like disease after *in vivo* passage in rhesus monkeys. *J Virol* 1996;70:6922–6928.
24. Pawar SN, Mattila JT, Sturgeon TJ, Lin PL, Narayan O, Montelaro RC, Flynn JL. Comparison of the effects of pathogenic simian human immunodeficiency virus strains SHIV-89.6P and SHIV-KU2 in cynomolgus macaques. *AIDS Res Hum Retroviruses* 2008;24:643–654.
25. Kling HM, Shipley TW, Patil S, Morris A, Norris KA. Pneumocystis colonization in immunocompetent and simian immunodeficiency virus–infected cynomolgus macaques. *J Infect Dis* 2009;199:89–96.
26. Segal J, Pearl RG, Ford AJ Jr, Stern RA, Gehlbach SM. Instantaneous and continuous cardiac output obtained with a Doppler pulmonary artery catheter. *J Am Coll Cardiol* 1989;13:1382–1392.

27. Matsuoka S, Washko GR, Yamashiro T, Estepar RS, Diaz A, Silverman EK, Hoffman E, Fessler HE, Criner GJ, Marchetti N, *et al*. Pulmonary hypertension and computed tomography measurement of small pulmonary vessels in severe emphysema. *Am J Respir Crit Care Med* 2010;181:218–225.
28. Shipley TW, Kling HM, Morris A, Patil S, Kristoff J, Guyach SE, Murphy JE, Shao X, Sciurba FC, Rogers RM, *et al*. Persistent pneumocystis colonization leads to the development of chronic obstructive pulmonary disease in a nonhuman primate model of AIDS. *J Infect Dis* 2010;202:302–312.
29. Champion HC, Michelakis ED, Hassoun PM. Comprehensive invasive and noninvasive approach to the right ventricle–pulmonary circulation unit: state of the art and clinical and research implications. *Circulation* 2009;120:992–1007.
30. Reimann KA, Parker RA, Seaman MS, Beaudry K, Beddall M, Peterson L, Williams KC, Veazey RS, Montefiori DC, Mascola JR, *et al*. Pathogenicity of simian–human immunodeficiency virus SHIV-89.6P and SIVmac is attenuated in cynomolgus macaques and associated with early T-lymphocyte responses. *J Virol* 2005;79:8878–8885.
31. Tanaka Y, Schuster DP, Davis EC, Patterson GA, Botney MD. The role of vascular injury and hemodynamics in rat pulmonary artery remodeling. *J Clin Invest* 1996;98:434–442.
32. Kanmogne GD, Primeaux C, Grammas P. Induction of apoptosis and endothelin-1 secretion in primary human lung endothelial cells by HIV-1 GP120 proteins. *Biochem Biophys Res Commun* 2005;333: 1107–1115.
33. Dhillon NK, Li F, Xue B, Tawfik O, Morgello S, Buch S, Ladner AO. Effect of cocaine on human immunodeficiency virus–mediated pulmonary endothelial and smooth muscle dysfunction. *Am J Respir Cell Mol Biol* 2011;45:40–52.
34. Lund AK, Lucero J, Herbert L, Liu Y, Naik JS. Human immunodeficiency virus transgenic rats exhibit pulmonary hypertension. *Am J Physiol Lung Cell Mol Physiol* 2011;301:L315–L326.
35. Kovacs G, Berghold A, Scheidl S, Olschewski H. Pulmonary arterial pressure during rest and exercise in healthy subjects: a systematic review. *Eur Respir J* 2009;34:888–894.
36. Kling HM, Shipley TW, Patil SP, Kristoff J, Bryan M, Montelaro RC, Morris A, Norris KA. Relationship of *Pneumocystis jiroveci* humoral immunity to prevention of colonization and chronic obstructive pulmonary disease in a primate model of HIV infection. *Infect Immun* 2010;78:4320–4330.
37. Ewalenko P, Brimioulle S, Delcroix M, Lejeune P, Naeije R. Comparison of the effects of isoflurane with those of propofol on pulmonary vascular impedance in experimental embolic pulmonary hypertension. *Br J Anaesth* 1997;79:625–630.
38. Ewalenko P, Stefanidis C, Holoye A, Brimioulle S, Naeije R. Pulmonary vascular impedance vs. resistance in hypoxic and hyperoxic dogs: effects of propofol and isoflurane. *J Appl Physiol* 1993;74:2188–2193.
39. Appay V, Sauce D. Immune activation and inflammation in HIV-1 infection: causes and consequences. *J Pathol* 2008;214:231–241.
40. Papagno L, Spina CA, Marchant A, Salio M, Rufer N, Little S, Dong T, Chesney G, Waters A, Easterbrook P, *et al*. Immune activation and $CD8^+$ T-cell differentiation towards senescence in HIV-1 infection. *PLoS Biol* 2004;2:E20.
41. Hunt PW, Martin JN, Sinclair E, Bredt B, Hagos E, Lampiris H, Deeks SG. T cell activation is associated with lower $CD4^+$ T cell gains in human immunodeficiency virus–infected patients with sustained viral suppression during antiretroviral therapy. *J Infect Dis* 2003;187:1534–1543.
42. Bosinger SE, Sodora DL, Silvestri G. Generalized immune activation and innate immune responses in simian immunodeficiency virus infection. *Curr Opin HIV AIDS* 2011;6:411–418.
43. Mermis J, Gu H, Xue B, Li F, Tawfik O, Buch S, Bartolome S, O'Brien-Ladner A, Dhillon NK. Hypoxia-inducible factor–1 alpha/platelet derived growth factor axis in HIV-associated pulmonary vascular remodeling. *Respir Res* 2011;12:103.